

# RESEARCH MEMORANDUM

DESIGN DATA FOR GRAPHICAL CONSTRUCTION  
OF TWO-DIMENSIONAL SHARP-EDGE-THROAT  
SUPERSONIC NOZZLES

By Harold Shames and Ferris L. Seashore

Lewis Flight Propulsion Laboratory  
Cleveland, Ohio

NATIONAL ADVISORY COMMITTEE  
FOR AERONAUTICS

WASHINGTON  
December 2, 1948

NACA RM E8J12

DESIGN DATA FOR GRAPHICAL CONSTRUCTION OF  
TWO-DIMENSIONAL SHARP-EDGE-THROAT SUPERSONIC NOZZLES  
By Harold Shames and Ferris L. Seashore

Release date December 2, 1948

In table 1 page 15, the  $\beta$  (column 3) value for  $\psi^-$  of .46 should be 19.99 instead of 19.90.

The  $\frac{y}{A_t/2}$  values (column 5) for  $\psi^-$  43.00, 45.00 and 47.00 should be 7.73, 5.77, and 1.80 instead of 3.87, 2.88, and .90.

NATIONAL ADVISORY COMMITTEE FOR AERONAUTICS

RESEARCH MEMORANDUM

DESIGN DATA FOR GRAPHICAL CONSTRUCTION  
OF TWO-DIMENSIONAL SHARP-EDGE-THROAT  
SUPERSONIC NOZZLES

By Harold Shames and Ferris I. Seashore

SUMMARY

Design data are presented for the graphical construction of two-dimensional sharp-edge-throat supersonic nozzles of minimum length for test-section Mach numbers from 1.20 to 10.00. The method of characteristics used in the design is briefly reviewed.

INTRODUCTION

A general discussion of the method of characteristics as applied to supersonic-nozzle design is given in references 1 to 3. The application of the method of characteristics to the design of minimum-length sharp-edge-throat nozzles is described in reference 3.

By means of charts and tables presented herein for designing such nozzles using an expansion "kernel," nozzle-wall contours for wind-tunnel test-section Mach numbers from 1.20 to 10.00 may be obtained with a minimum of graphical construction. The principles of the method of characteristics used in the design are reviewed. The nomenclature of reference 1 was found to be more convenient than the speed-index or pressure-number systems of references 2 and 3, and is therefore used in this report.

SYMBOLS

The following symbols are used in this report:

- $A_F$  area of nozzle bearing uniform flow at  $M_F$  (equal to height for nozzle of unit width)
- $A_t$  area of nozzle at throat (equal to height for nozzle of unit width)

- L length of nozzle from throat to test section
- $l_k$  length of kernel
- M Mach number
- $M_F$  final Mach number
- x abscissa of point of intersection of  $\psi_F^+$  characteristic with  $\psi^-$  characteristic
- y ordinate of point of intersection of  $\psi_F^-$  characteristic with  $\psi^-$  characteristic
- $\alpha$  angle of wall to nozzle axis
- $\beta$  Mach angle,  $\left(\sin^{-1} \frac{1}{M}\right)$
- $\beta_F$  final Mach angle
- $\gamma$  ratio of specific heat at constant pressure to specific heat at constant volume
- $\theta$  angle of inclination of streamline to nozzle axis
- $\lambda^+$  angle that  $\psi^+$  characteristic makes with x axis ( $\beta - \theta$ )  
( $\lambda^+$  is positive number when drawn below horizontal)
- $\lambda^-$  angle that  $\psi^-$  characteristic makes with x axis ( $\beta + \theta$ )  
( $\lambda^-$  is positive number when drawn above horizontal)
- $\varphi$  angle of corner in wall at nozzle throat
- $\psi$  equivalent Prandtl-Meyer turning angle
- $\psi^+$  characteristics (Mach waves) originating at upper nozzle wall
- $\psi^-$  characteristics (Mach waves) originating at lower nozzle wall
- $\psi_F$  value of  $\psi$  at nozzle exit
- $\psi_F^+$  downstream characteristic bounding expansion wave originating at upper nozzle wall
- $\psi_F^-$  downstream characteristic bounding expansion wave originating at lower nozzle wall

## METHOD OF NOZZLE DESIGN

## System of Characteristics in Sharp-Edge-Throat Nozzles

986

A two-dimensional nozzle with a sharp-edge throat is shown in figure 1. The increase in flow Mach number with displacement downstream of the throat is obtained from the system of expansion waves generated at the angular turn of the wall at the nozzle throat (fig. 2(a)). The expansion waves, as shown in figure 2(a), turn the flow toward the adjacent nozzle wall downstream of the corner with a consequent increase in stream-tube cross-sectional area and Mach number. The system of expansion waves from each corner is identical with that developed in an infinite uniform sonic flow constrained to flow around a sharp corner in a single two-dimensional wall. The solution for this case is discussed in reference 4. The expansion waves are propagated into the flow along straight lines radiating from the corner in the case for the flow along only one wall in an infinite flow. Along any given radial line, the flow direction, the Mach number, and the physical state of the gas is the same for all points on that line (fig. 2(a)). Each of these radial lines can be assigned a number in degrees or radians that corresponds to the angular deviation of the flow crossing the line from the direction of the undisturbed sonic flow. A line so numbered is called a characteristic. The angular deviation of the flow between two characteristics is equal to the difference of the numbers assigned to these characteristics. At each characteristic, the flow makes the Mach angle  $\beta = \sin^{-1} 1/M$  with the characteristic. The characteristics are therefore coincident with the Mach lines in the flow.

Two separate walls in the flow (fig. 2(a)) result in two separate systems of intersecting expansion waves originating at the respective wall corners. If the characteristics from the upper and lower walls are designated  $\psi^+$  and  $\psi^-$ , respectively, every point in the flow traversed by both expansion waves is crossed by a characteristic from the upper and lower walls. Because of the simultaneous influence on the flow of the expansion waves from the corner on the upper and lower walls in the zone common to both sets of waves, the characteristics are curved to maintain the Mach angle with the flow (zone I, fig. 2(b)). The characteristics are straight in zones occupied by only one set of expansion waves (zones II and III, fig. 2(b)).

By means of the characteristics in zones II and III, the graphical construction of the nozzle-wall contour required to

give wave-free flow in the test section can be made. Tables I and II provide the information for obtaining the characteristics in zones II and III without involved plotting or computation. The construction of the wave pattern from which the information in tables I and II was obtained is described in the following section.

#### Development of Kernel

From references 2 and 4, the value of the flow Mach number at a point in the flow, crossed by characteristics having values of  $\psi^+$  and  $\psi^-$ , respectively, is given by

$$\psi = \psi^+ + \psi^- = \sqrt{\frac{\gamma+1}{\gamma-1}} \tan^{-1} \frac{\sqrt{M^2-1}}{\sqrt{\frac{\gamma+1}{\gamma-1}}} - \tan^{-1} \sqrt{M^2-1} \quad (1)$$

The flow direction with respect to the nozzle axis is

$$\theta = \psi^+ - \psi^- \quad (2)$$

For an isentropic flow of known uniform total pressure and temperature, the flow at any point is completely specified by the local values of the intersecting pair of characteristics.

A wave pattern for a pair of opposite corners at the nozzle throat is established by dividing the wave emitted by each corner into a convenient number of characteristics, and by determining the resulting wave pattern due to the interaction of both sets of waves by means of the foregoing principles; that is, the local Mach number is given by equation (1), the flow direction is given by equation (2), and the local Mach angle is determined from the relation  $\beta = \sin^{-1} 1/M$ .

The resulting system of characteristics in the zone of the flow traversed by waves from both corners (zone I, fig. 2(b)) is shown schematically in figure 2(c). Such a pattern is called a kernel. In order to obtain the tables giving the pertinent design parameters for sharp-edge nozzles ranging in test-section Mach number from 1.20 to 10.00, a kernel was graphically developed for two opposing corners of equal angle ( $51.16^\circ$ ) corresponding to  $M = 10.00$  at the test section with the following increments in  $\psi^+$  and  $\psi^-$ :

$\psi^+$ and $\psi^-$ limits (deg)	$\psi^+$ and $\psi^-$ increments (deg)
0 - 0.01	0.01
.01 - .19	.03
.19 - .37	.06
.37 - 1.00	.09
1.00 - 2.00	.20
2.00 - 4.00	.40
4.00 - 8.00	.50
8.00 - 19.00	1.00
19.00 - 51.16	2.00

In the range of low values of  $\psi^+$  and  $\psi^-$ , where the construction is sensitive to small changes in these values, small increments in  $\psi^+$  and  $\psi^-$  were used, as indicated in the preceding table.

Because the corners at the nozzle throat were chosen equal, the resultant wave pattern is symmetrical and only the half above the nozzle axis need be considered. The wave pattern at any point in the kernel is not influenced by the wave pattern downstream of that point. Consequently, the kernel for any corner less than the maximum of  $51.16^\circ$  can be obtained from the kernel for  $51.16^\circ$  by neglecting the characteristics of value greater than the desired corner angle. This principle is illustrated in figure 2(c).

The bounding characteristic separating zone I from zone II (fig. 2(b)) is designated as  $\psi_f^+$ . The points of intersection of the  $\psi^-$  characteristics with the  $\psi_f^+$  characteristic, and the slopes of the  $\psi^-$  characteristics at these points, are all that is required to determine the nozzle contour.

The constructed kernel for  $M = 10.00$  provided data for the design of nozzles for final Mach numbers  $M_f$  from 1.20 to 2.00 in increments of 0.20 and from 2.00 to 10.00 in increments of 1.00.

The coordinates  $\left(\frac{x}{A_t/2}, \frac{y}{A_t/2}\right)$  of the points of intersection of the bounding characteristic  $\psi_f^+$  with the  $\psi^-$  characteristics are tabulated with other pertinent data in table I.

For Mach numbers up to 4.00, a kernel of 12-inch half throat height  $A_t/2$  was graphically developed and for Mach numbers from 5.00 to 10.00 a half throat height of 6 inches was used. For the

6-inch kernel, however, the scale was reduced at intervals as the height of the kernel increased in order to maintain the construction within the physical limit of the drawing board. This scale reduction accounts for the decreasing number of decimal places for the coordinates in table I in the high Mach number range. Turning-angle increments in  $\psi^+$  and  $\psi^-$ , as given in the preceding table, were used for both kernels. Construction was performed with a drafting machine capable of setting to  $\pm 2.5$  minutes.

### Wall Contour

An expansion wave incident on a channel wall will, in general, require that a secondary wave be emitted at the point of incidence in order to keep the flow against the wall. If the wall is curved in the way a streamline would be turned under the influence of the incident wave, however, no secondary wave arises to keep the flow along the wall. This method of suppression of secondary waves is the principle used to obtain uniform wave-free flow in the test section. The graphical construction is required to locate the point of incidence of the waves on the nozzle wall. The difference in value of the characteristics bounding the incident wave gives the change of wall inclination required to suppress secondary waves (fig. 2(d)); that is, for the upper wall,

$$\Delta\alpha = \Delta\psi^- \quad (3a)$$

or for the lower wall,

$$\Delta\alpha = \Delta\psi^+ \quad (3b)$$

where  $\Delta\alpha$  is the required change of wall inclination. The accuracy of the wall contour obtained improves as the number of characteristics drawn to represent the incident expansion wave is increased. Only the upper nozzle wall need be developed if the nozzle is symmetrical about the center line.

Symmetrical two-dimensional sharp-edge-throat nozzles are produced by making the angle of the turn at both walls at the throat equal in magnitude. If  $\phi$  represents the angle of turn for the upper and lower walls, the downstream characteristics  $\psi_F^+$  and  $\psi_F^-$  that bound the respective expansion waves will have this value.

Because of the symmetry of the wave pattern about the nozzle axis, a  $\psi^+$  characteristic will intersect a  $\psi^-$  characteristic of the same magnitude at the nozzle axis. In particular, the  $\psi_F^+$  and  $\psi_F^-$



characteristics intersect on the nozzle axis (fig. 2(c)). The flow along the streamline on the nozzle axis will have the final Mach number  $M_f$  at the intersection of these bounding characteristics. From equation (1),

$$\psi_f^+ + \psi_f^- = \psi_f = \sqrt{\frac{\gamma+1}{\gamma-1}} \tan^{-1} \frac{\sqrt{M_f^2-1}}{\sqrt{\frac{\gamma+1}{\gamma-1}}} - \tan^{-1} \sqrt{M_f^2-1}$$

Because  $\psi_f^+$  and  $\psi_f^-$  are equal in magnitude and represent the angle through which each wall is turned at the throat,

$$\varphi = \psi_f^+ = \psi_f^- = \frac{\psi_f}{2} = \frac{1}{2} \sqrt{\frac{\gamma+1}{\gamma-1}} \tan^{-1} \frac{\sqrt{M_f^2-1}}{\sqrt{\frac{\gamma+1}{\gamma-1}}} - \tan^{-1} \sqrt{M_f^2-1} \quad (4)$$

Equation (4) gives the value of the wall angle at the throat that corresponds to the desired test-section Mach number  $M_f$ . These values are presented in table II, columns 1 and 2.

The method of using the kernel that is schematically shown in figure 3(a) to obtain the nozzle-wall contour of two-dimensional sharp-throat nozzles of minimum length (fig. 3(b)) is illustrated by application to a specific problem. Assume that it is desired to design a nozzle of this class with a test-section Mach number of 4.00 and a throat height of 6 inches.

The throat-corner angle  $\varphi$  and the value of the downstream bounding characteristics  $\psi_f^+$  are obtained from equation (4) or table II, column 2, with  $M_f$  equal to 4.00, column 1:

$$\varphi = \psi_f^+ = \psi_f^- = 32.89^\circ$$

The wall contour is obtained by plotting the zone II characteristics of the  $\psi^-$  set (fig. 3(b)), which are straight lines that make the angle  $\lambda^-$  with the nozzle axis at the intersection of the  $\psi^-$  characteristics and the bounding characteristic  $\psi_f^+$ . All that is required to obtain the zone II plot are the coordinates of the points

of intersection of the  $\psi^-$  set of characteristics with the bounding characteristic  $\psi_F^+$  and the local slopes  $\lambda^-$  of the  $\psi^-$  characteristics. Columns 4 and 5 of table I give the coordinates of intersection in terms of the half throat height  $A_t/2$  and column 6 gives the angle of inclination  $\lambda^-$  of the  $\psi^-$  characteristic at the intersection. For example, the  $\psi^- = 12.00^\circ$  characteristic

intersects the  $\psi_F^+$  characteristic at  $\frac{x}{A_t/2} = 3.453$  and  $\frac{y}{A_t/2} = 1.256$ , which gives  $x = 10.359$  and  $y = 3.768$  for a nozzle

of 6-inch throat. The inclination of the  $\psi^-$  characteristic in zone II is  $\lambda^- = 42.14^\circ$ . The complete plot of the zone II characteristics has the form schematically illustrated in figure 4(a).

Construction of the nozzle wall starts at the nozzle throat with a straight-line segment  $ab$  (fig. 4(b)) that makes the angle with the nozzle axis  $\varphi = 32.89^\circ$ , which was previously computed for  $M_F = 4.00$ . At the intersection of the nozzle wall with the first  $\psi^-$  characteristic ( $\psi_1^- = 0.01^\circ$ ), the inclination of the wall is reduced according to equation (3a) by an amount  $(\psi_1^- - \psi_0^-)$  corresponding to the angle through which the flow is turned clockwise by the expansion wave between  $\psi_0^-$  and  $\psi_1^-$ . As previously discussed, no wave emission occurs at the wall turned in this way. At every intersection of the wall with a characteristic, the wall inclination to the nozzle axis is reduced by the angle of turning produced by the wave between  $\psi_n^-$  and  $\psi_{n-1}^-$ . The angle of the wall  $\alpha$  at each characteristic is given in table I, column 7. For example, at point  $b$ ,  $\psi^- = 0.01^\circ$  and  $\alpha = 32.88^\circ$ ; similarly at point  $c$ ,  $\psi^- = 0.04^\circ$  and  $\alpha = 32.85^\circ$ . When the sequence of straight-line segments representing the nozzle wall is completed, a smooth curve approximating the shape of the sequence of straight lines is taken as the effective nozzle-wall contour. The accuracy of the final wall contour increases with the number of characteristics used to represent the expansion waves from the wall corners at the nozzle throat.

An averaging method for attaining a contour that is closer to the true contour will be described for a nozzle with a test-section Mach number  $M_F$  of 4.00 as an example, as shown in figure 4(b). As before, construction starts at the nozzle throat with a straight line  $ab$  making the corner angle with the nozzle axis ( $\varphi = 32.89^\circ$ ). Line  $ab$  is then bisected by point  $c$ , and line  $cd$  is drawn at the wall angle  $\alpha = 32.88^\circ$ , corresponding to  $\psi^- = 0.01^\circ$ , (table I, column 7) until it intersects the  $\psi^- = 0.04^\circ$  characteristic.

Point B, the wall coordinate point lying along  $\psi^- = 0.01^\circ$ , is located by the intersection of line *od* and  $\psi^- = 0.01^\circ$ . Line *Bd* is then bisected by point *e*, and line *eg* is drawn at the wall angle  $\alpha = 32.85^\circ$  corresponding to  $\psi^- = 0.04^\circ$ . Point *D* is located by the intersection of line *eg* and  $\psi^- = 0.04^\circ$ . The preceding process is continued until the design is complete. The nozzle contour is taken as the smooth curve through points *a, B, D, . . .*, tangent to construction lines *ab, cd, eg, . . .*.

The test-section height of the nozzle (numerically equal to  $A_f$ ), which is obtained by either of the graphical processes described, should be related to the throat height by the expression

$$\frac{A_f}{A_t} = \frac{1}{M_f} \left( \frac{1 + \frac{\gamma-1}{2} M_f^2}{\frac{\gamma+1}{2}} \right)^{\frac{\gamma+1}{2(\gamma-1)}} \quad (5)$$

These area-ratio values are presented in table II, column 4. For example, for  $M_f = 4.00$ ,  $\frac{A_f}{A_t} = 10.719$ .

The design of a nozzle that has a Mach number intermediate between values given in table I requires the determination of the shape of the  $\psi_f^+$  characteristic of the kernel corresponding to the desired Mach number. This design is accomplished by using the coordinates of the  $\psi_f^+$  characteristic given in table I that are closest to the desired Mach number and then establishing by construction the points of intersection of the  $\psi_f^+$  characteristics that correspond to the desired Mach number with the  $\psi^-$  characteristics, as shown in figure 5. For example, the kernel for  $M = 4.30$  is established with the kernel for  $M = 4.00$  as a base.

The bounding characteristic  $\psi_f^+$  and the zone II plot of  $\psi^-$  characteristics for  $M_f = 4.00$  are established as previously described. These characteristics are dashed in figure 5. The bounding characteristic and the zone II plot of  $\psi^-$  characteristics for  $M_f = 4.30$  are established according to the following procedure:

The value of the bounding characteristic  $\psi_f^+$  for  $M_f = 4.30$  is obtained from equation (4) or table II, column 2, ( $\psi_f^+ = 34.77^\circ$ ).

The angle that the  $\psi_f^+$  characteristic makes with the nozzle axis at any point is designated  $\psi^+$  (fig. 5) and is determined by the relation

$$\lambda^+ = \beta - \theta \quad (6)$$

where  $\beta$  is the Mach angle determined by the local Mach number corresponding to the local equivalent Prandtl-Meyer turning angle  $\psi$ , given by equation (1), and  $\theta$  is the angle of inclination of the flow to the nozzle axis, given by equation (2). (Note that positive values of  $\lambda^+$  are drawn with a negative slope.) Thus at point A at the throat (fig. 5):

from equation (1),

$$\psi = \psi^+ + \psi^- = 34.77 + 0 = 34.77^\circ$$

from table II, columns 3 and 5, for  $\psi = 34.77$ ,

$$\beta = 25.53^\circ$$

from equation (2),

$$\theta = \psi^+ - \psi^- = 34.77 - 0 = 34.77^\circ$$

Consequently,

$$\lambda^+ = \beta - \theta = 25.53 - 34.77 = -9.24^\circ$$

The negative sign indicates that  $\lambda^+$  is drawn with positive slope, as shown at point A of figure 5. The bounding  $\psi_f^+$  characteristic is drawn at the angle  $\lambda^+ = -9.24^\circ$ , until it intersects the first  $\psi^-$  characteristic  $\psi^- = 0.01^\circ$  at point B. At point B the new  $\lambda^+$  value for  $\psi_f^+$  is determined by repeating the aforementioned procedure using  $\psi^+ = 34.77^\circ$  and  $\psi^- = 0.01^\circ$ . The  $\psi_f^+$  characteristic is drawn at this new  $\lambda^+$  value until it intersects the next  $\psi^-$  characteristic  $\psi^- = 0.04^\circ$ . The slope of the  $\psi^-$  characteristic at point B,  $\lambda^-$ , is determined by the relation (fig. 5)

$$\lambda^- = \beta + \theta \quad (7)$$

with the same values for  $\beta$  and  $\theta$  as were used to determine  $\lambda^+$ . In this manner the entire zone II plot of  $\psi^-$  characteristics is obtained for  $M_f = 4.30$ .

The wall contour is then developed by the method previously described for  $M_p = 4.00$ . The entire procedure is expedited if columns 1 to 3, 6, and 7,  $\phi$  and  $\psi_F^+$ , of table I, and  $\lambda^+$  are determined for the  $\psi_F^+$  characteristic for  $M = 4.30$  before the drawing is initiated.

### Nozzle Length

The nozzle length from the throat to the test section may be calculated from the length of the kernel and the projection of the last characteristic on the nozzle axis, as shown in figure 3(b). The projection may be determined from the final Mach angle and the final area ratio. The expression for the ratio of the nozzle length to the nozzle test-section height

$$\frac{L}{A_F} = \left( \frac{l_k}{A_t} + \frac{A_F}{2A_t \tan \beta} \right) \frac{A_t}{A_F}$$

is plotted in figure 6 for Mach numbers up to 10.

Lewis Flight Propulsion Laboratory,  
National Advisory Committee for Aeronautics,  
Cleveland, Ohio.

### REFERENCES

1. Pinkel, I. Irving: Equations for the Design of Two-Dimensional Supersonic Nozzles. NACA RM No. E8B02, 1948.
2. Puckett, A. E.: Supersonic Nozzle Design. Jour. Appl. Mech., vol. 13, no. 4, Dec. 1946, pp. A265-A270.
3. Shapiro, Ascher H., and Edelman, Gilbert M.: Method of Characteristics for Two-Dimensional Supersonic Flow - Graphical and Numerical Procedures. Jour. Appl. Mech., vol. 14, no. 2, June 1947, pp. A154-A162.
4. Taylor, G. I., and Maccoll, J. W.: The Two-Dimensional Flow Around a Corner; Two-Dimensional Flow Past a Curved Surface. Vol. III of Aerodynamic Theory, div. H, ch. IV, secs. 5-6, W. F. Durand, ed., Julius Springer (Berlin), 1935, pp. 243-249.

TABLE I. - DETAILED NOZZLE DESIGN PARAMETERS  
 $\gamma = 1.400$

1	2	3	4	5	6	7	1	2	3	4	5	6	7
$\gamma^-$ (deg)	$\gamma$ (deg)	$\beta$ (deg)	$\frac{x}{A_t/2}$	$\frac{y}{A_t/2}$	$\lambda^-$ (deg)	$\alpha$ (deg)	$\gamma^-$ (deg)	$\gamma$ (deg)	$\beta$ (deg)	$\frac{x}{A_t/2}$	$\frac{y}{A_t/2}$	$\lambda^-$ (deg)	$\alpha$ (deg)
$M_F, 1.20; \phi$ and $\gamma_F^+, 1.80^\circ$							0.51	7.81	47.41	0.557	0.525	54.60	7.19
0	1.80	62.91	0	1.000	—	1.80	.37	7.87	47.32	.577	.508	54.45	7.13
.01	1.81	62.87	.213	.614	64.66	1.79	.46	7.96	47.17	.600	.489	54.21	7.04
.04	1.84	62.72	.277	.600	64.48	1.76	.53	8.06	47.03	.622	.471	53.98	6.95
.07	1.87	62.59	.305	.448	64.32	1.73	.64	8.14	46.89	.643	.454	53.75	6.86
.10	1.90	62.45	.328	.408	64.15	1.70	.73	8.23	46.75	.661	.439	53.52	6.77
.13	1.93	62.32	.343	.380	63.99	1.67	.82	8.32	46.61	.679	.425	53.29	6.68
.16	1.96	62.18	.356	.357	63.82	1.64	.91	8.41	46.47	.694	.412	53.06	6.59
.19	1.99	62.05	.368	.338	63.66	1.61	1.00	8.50	46.33	.708	.399	52.83	6.50
.25	2.05	61.78	.386	.305	63.33	1.55	1.20	8.70	46.03	.738	.375	52.33	6.30
.31	2.11	61.52	.404	.274	63.01	1.49	1.40	8.90	45.73	.764	.353	51.83	6.10
.37	2.17	61.28	.417	.253	62.71	1.43	1.60	9.10	45.43	.787	.333	51.33	5.90
.46	2.26	60.89	.433	.223	62.23	1.34	1.80	9.30	45.14	.810	.315	50.84	5.70
.55	2.35	60.53	.448	.198	61.78	1.25	2.00	9.50	44.85	.828	.300	50.35	5.50
.64	2.44	60.19	.463	.176	61.34	1.18	2.40	9.90	44.32	.867	.268	49.42	5.10
.73	2.53	59.84	.475	.155	60.91	1.07	2.80	10.30	43.78	.903	.239	48.48	4.70
.82	2.62	59.50	.487	.136	60.48	.98	3.20	10.70	43.28	.934	.213	47.58	4.50
.91	2.71	59.18	.498	.118	60.07	.89	3.60	11.10	42.80	.963	.190	46.70	3.90
1.00	2.80	58.86	.507	.103	59.66	.80	4.00	11.50	42.30	.992	.167	45.80	3.50
1.20	3.00	58.18	.527	.072	58.78	.60	4.50	12.00	41.72	1.022	.142	44.72	3.00
1.40	3.20	57.57	.543	.046	57.97	.40	5.00	12.50	41.15	1.054	.117	43.65	2.50
1.60	3.40	56.98	.559	.022	57.18	.20	5.50	13.00	40.60	1.083	.093	42.60	2.00
1.80	3.60	56.40	.574	0	56.40	0	6.00	13.50	40.05	1.115	.067	41.55	1.60
$M_F, 1.40; \phi$ and $\gamma_F^+, 4.50^\circ$							6.50	14.00	39.53	1.145	.045	40.53	1.00
0	4.50	53.99	0	1.000	—	4.50	7.00	14.50	39.04	1.172	.022	39.54	.50
.01	4.51	53.97	.257	.698	58.46	4.49	7.50	15.00	38.54	1.202	0	38.54	0
.04	4.54	53.89	.335	.607	58.35	4.46	$M_F, 1.80; \phi$ and $\gamma_F^+, 10.36^\circ$						
.07	4.57	53.82	.369	.567	58.25	4.43	0	10.36	43.70	0	1.000	—	10.36
.10	4.60	53.75	.397	.535	58.15	4.40	.01	10.37	43.69	.320	.790	54.04	10.35
.13	4.63	53.68	.417	.513	58.05	4.37	.04	10.40	43.65	.417	.725	53.97	10.32
.16	4.66	53.60	.432	.495	57.94	4.34	.07	10.43	43.61	.480	.697	53.90	10.29
.19	4.69	53.53	.447	.477	57.84	4.31	.10	10.46	43.57	.494	.675	53.83	10.26
.25	4.75	53.38	.469	.452	57.63	4.25	.13	10.49	43.53	.517	.659	53.76	10.23
.31	4.81	53.23	.491	.427	57.42	4.19	.16	10.52	43.50	.537	.646	53.70	10.20
.37	4.87	53.08	.507	.407	57.21	4.13	.19	10.55	43.46	.557	.633	53.63	10.17
.46	4.96	52.87	.527	.384	56.91	4.04	.25	10.61	43.39	.583	.615	53.50	10.11
.55	5.05	52.66	.547	.363	56.61	3.95	.31	10.67	43.32	.612	.597	53.37	10.05
.64	5.14	52.46	.564	.342	56.32	3.86	.37	10.73	43.24	.632	.583	53.23	9.99
.73	5.23	52.26	.580	.325	56.03	3.77	.46	10.82	43.14	.658	.567	53.04	9.90
.82	5.32	52.06	.594	.308	55.74	3.68	.55	10.91	43.03	.682	.550	52.84	9.81
.91	5.41	51.86	.606	.293	55.45	3.59	.64	11.00	42.92	.704	.535	52.64	9.72
1.00	5.50	51.66	.620	.279	55.16	3.50	.73	11.09	42.81	.725	.522	52.44	9.63
1.20	5.70	51.25	.645	.252	54.55	3.30	.82	11.18	42.70	.743	.510	52.24	9.54
1.40	5.90	50.83	.667	.227	53.93	3.10	.91	11.27	42.59	.762	.498	52.04	9.45
1.60	6.10	50.43	.687	.205	53.33	2.90	1.00	11.36	42.47	.777	.488	51.83	9.36
1.80	6.30	50.05	.706	.185	52.75	2.70	1.20	11.56	42.23	.811	.467	51.39	9.16
2.00	6.50	49.66	.722	.167	52.16	2.50	1.40	11.76	42.00	.841	.447	50.96	8.96
2.40	6.90	48.93	.752	.133	51.03	2.10	1.60	11.96	41.77	.867	.430	50.53	8.76
2.80	7.30	48.24	.783	.101	49.94	1.70	1.80	12.16	41.54	.892	.413	50.10	8.56
3.20	7.70	47.58	.808	.075	48.88	1.30	2.00	12.36	41.31	.912	.400	49.67	8.36
3.60	8.10	46.95	.832	.050	47.85	.90	2.40	12.76	40.86	.957	.371	48.82	7.96
4.00	8.50	46.33	.856	.025	46.83	.50	2.80	13.16	40.42	.997	.345	47.98	7.56
4.50	9.00	45.57	.880	0	45.57	0	3.20	13.56	39.99	1.034	.321	47.15	7.16
$M_F, 1.60; \phi$ and $\gamma_F^+, 7.50^\circ$							3.60	13.96	39.57	1.067	.300	46.33	6.76
0	7.50	47.90	0	1.000	—	7.50	4.00	14.36	39.18	1.102	.277	45.54	6.36
.01	7.51	47.88	.292	.761	55.37	7.49	4.50	14.86	38.68	1.137	.254	44.54	5.86
.04	7.54	47.84	.381	.676	55.30	7.46	5.00	15.36	38.21	1.175	.231	43.57	5.36
.07	7.57	47.79	.421	.642	55.22	7.43	5.50	15.86	37.76	1.208	.208	42.62	4.86
.10	7.60	47.74	.451	.616	55.14	7.40	6.00	16.36	37.30	1.247	.183	41.66	4.36
.13	7.63	47.69	.472	.597	55.06	7.37	6.50	16.86	36.86	1.282	.162	40.72	3.86
.16	7.66	47.64	.492	.582	54.98	7.34	7.00	17.36	36.42	1.315	.139	39.78	3.36
.19	7.69	47.60	.508	.567	54.91	7.31	7.50	17.86	36.00	1.350	.117	38.86	2.86
.25	7.75	47.50	.533	.546	54.75	7.25	8.00	18.36	35.59	1.379	.097	37.95	2.36
							9.00	19.36	34.80	1.443	.055	36.16	1.36
							10.00	20.36	34.04	1.507	.012	34.40	.36
							10.36	20.72	33.76	1.528	0	33.76	0

TABLE I. - DETAILED NOZZLE DESIGN PARAMETERS - Continued

 $[\gamma = 1.400]$ 

1	2	3	4	5	6	7	1	2	3	4	5	6	7
$\gamma^-$ (deg)	$\gamma$ (deg)	$\beta$ (deg)	$\frac{x}{A_t/2}$	$\frac{y}{A_t/2}$	$\lambda^-$ (deg)	$\alpha$ (deg)	$\gamma^-$ (deg)	$\gamma$ (deg)	$\beta$ (deg)	$\frac{x}{A_t/2}$	$\frac{y}{A_t/2}$	$\lambda^-$ (deg)	$\alpha$ (deg)
$M_F, 2.00; \phi$ and $\gamma_F^+, 15.19^\circ$							2.00	26.88	29.71	1.298	0.858	52.59	22.88
0	13.19	40.38	0	1.000	-----	13.19	2.40	27.28	29.48	1.368	.850	51.96	22.48
.01	13.20	40.38	.345	.824	53.56	13.18	2.80	27.68	29.24	1.434	.842	51.32	22.08
.04	13.23	40.35	.449	.770	53.50	13.15	3.20	28.08	29.01	1.496	.833	50.69	21.68
.07	13.26	40.31	.496	.746	53.43	13.12	3.60	28.48	28.79	1.555	.825	50.07	21.28
.10	13.29	40.27	.533	.728	53.36	13.09	4.00	28.88	28.56	1.616	.819	49.44	20.88
.13	13.32	40.25	.567	.715	53.31	13.06	4.50	29.38	28.29	1.678	.810	48.67	20.38
.16	13.35	40.22	.580	.703	53.25	13.03	5.00	29.88	28.03	1.745	.800	47.91	19.88
.19	13.38	40.18	.601	.692	53.18	13.00	5.50	30.38	27.75	1.812	.792	47.13	19.38
.25	13.44	40.12	.630	.678	53.06	12.94	6.00	30.88	27.47	1.883	.780	46.35	18.88
.31	13.50	40.05	.660	.662	52.93	12.88	6.50	31.38	27.22	1.949	.771	45.60	18.38
.37	13.56	39.99	.683	.650	52.81	12.82	7.00	31.88	26.96	2.015	.761	44.84	17.88
.46	13.65	39.89	.710	.637	52.62	12.73	7.50	32.38	26.71	2.085	.750	44.09	17.38
.55	13.74	39.80	.737	.622	52.44	12.64	8.00	32.88	26.46	2.147	.739	43.34	16.88
.64	13.83	39.71	.762	.609	52.26	12.55	9.00	33.88	25.97	2.281	.717	41.85	15.88
.73	13.92	39.61	.784	.609	52.07	12.46	10.00	34.88	25.49	2.417	.693	40.37	14.88
.82	14.01	39.52	.804	.588	51.89	12.37	11.00	35.88	25.04	2.554	.667	38.92	13.88
.91	14.10	39.43	.824	.578	51.71	12.28	12.00	36.88	24.59	2.695	.639	37.47	12.88
1.00	14.19	39.34	.842	.569	51.53	12.19	13.00	37.88	24.12	2.835	.611	36.00	11.88
1.20	14.39	39.15	.878	.550	51.14	11.99	14.00	38.88	23.69	2.982	.578	34.57	10.88
1.40	14.59	38.95	.911	.533	50.74	11.79	15.00	39.88	23.27	3.138	.543	33.15	9.88
1.60	14.79	38.75	.939	.519	50.34	11.59	16.00	40.88	22.85	3.289	.508	31.73	8.88
1.80	14.99	38.55	.958	.504	49.94	11.39	17.00	41.88	22.43	3.457	.467	30.31	7.88
2.00	15.19	38.37	.992	.492	49.56	11.19	18.00	42.88	22.03	3.618	.423	28.91	6.88
2.40	15.59	38.00	1.041	.467	48.79	10.79	19.00	43.88	21.64	3.796	.375	27.52	5.88
2.80	15.99	37.64	1.088	.443	48.03	10.39	21.00	45.88	20.88	4.167	.272	24.76	3.88
3.20	16.39	37.27	1.128	.422	47.26	9.99	23.00	47.88	20.14	4.584	.144	22.02	1.88
3.60	16.79	36.92	1.167	.403	46.51	9.59	24.88	49.76	19.47	5.023	0	19.47	0
4.00	17.19	36.65	1.206	.382	45.84	9.19	$M_F, 4.00; \phi$ and $\gamma_F^+, 32.89^\circ$						
4.50	17.59	36.14	1.246	.362	44.83	8.69	0	32.89	26.46	0	1.000	-----	32.89
5.00	18.19	35.73	1.288	.339	43.92	8.19	.01	32.90	26.45	.507	1.056	59.33	32.88
5.50	18.69	35.33	1.328	.318	43.02	7.69	.04	32.93	26.43	.661	1.073	59.28	32.85
6.00	19.19	34.93	1.373	.295	42.12	7.19	.07	32.96	26.42	.731	1.080	59.24	32.82
6.50	19.69	34.55	1.413	.274	41.24	6.69	.10	32.99	26.40	.785	1.088	59.19	32.79
7.00	20.19	34.17	1.453	.253	40.36	6.19	.13	33.02	26.39	.822	1.090	59.15	32.76
7.50	20.69	33.86	1.493	.232	39.55	5.69	.16	33.05	26.37	.857	1.094	59.10	32.73
8.00	21.19	33.41	1.528	.213	38.60	5.19	.19	33.08	26.36	.887	1.097	59.06	32.70
9.00	22.19	32.70	1.603	.173	36.89	4.19	.25	33.14	26.33	.931	1.102	58.97	32.64
10.00	23.19	32.01	1.679	.133	35.20	3.19	.31	33.20	26.30	.977	1.107	58.88	32.58
11.00	24.19	31.36	1.753	.092	33.56	2.19	.37	33.26	26.27	1.012	1.112	58.79	32.52
12.00	25.19	30.74	1.827	.052	31.93	1.19	.46	33.35	26.22	1.053	1.116	58.65	32.43
13.00	26.19	30.12	1.898	.012	30.31	.19	.55	33.44	26.18	1.096	1.120	58.52	32.34
13.19	26.38	30.00	1.918	0	30.00	0	.64	33.53	26.13	1.137	1.125	58.38	32.25
$M_F, 3.00; \phi$ and $\gamma_F^+, 24.86^\circ$							.73	33.62	26.09	1.172	1.129	58.25	32.16
0	24.88	30.92	0	1.000	-----	24.88	.82	33.71	26.04	1.204	1.132	58.11	32.07
.01	24.89	30.92	.439	.953	55.79	24.87	.91	33.80	26.01	1.235	1.135	57.99	31.98
.04	24.92	30.90	.573	.939	55.74	24.84	1.00	33.89	25.96	1.264	1.138	57.85	31.89
.07	24.95	30.88	.633	.928	55.69	24.81	1.20	34.09	25.86	1.326	1.145	57.55	31.69
.10	24.98	30.87	.681	.928	55.65	24.78	1.40	34.29	25.76	1.380	1.150	57.25	31.49
.13	25.01	30.85	.713	.925	55.60	24.75	1.60	34.49	25.66	1.427	1.155	56.95	31.29
.16	25.04	30.82	.742	.921	55.54	24.72	1.80	34.69	25.57	1.479	1.160	56.66	31.09
.19	25.07	30.81	.768	.918	55.50	24.69	2.00	34.89	25.48	1.522	1.164	56.37	30.89
.25	25.13	30.77	.805	.914	55.40	24.63	2.40	35.29	25.30	1.608	1.172	55.79	30.49
.31	25.19	30.73	.845	.910	55.30	24.57	2.80	35.69	25.12	1.694	1.180	55.21	30.09
.37	25.25	30.69	.875	.906	55.20	24.51	3.20	36.09	24.95	1.772	1.187	54.64	29.69
.46	25.34	30.64	.909	.903	55.06	24.42	3.60	36.49	24.77	1.849	1.192	54.06	29.29
.55	25.43	30.58	.946	.898	54.91	24.33	4.00	36.89	24.68	1.927	1.199	53.47	28.89
.64	25.52	30.53	.980	.895	54.77	24.24	4.50	37.39	24.54	2.011	1.205	52.73	28.39
.73	25.61	30.47	1.010	.892	54.62	24.15	5.00	37.89	24.41	2.099	1.212	52.00	27.89
.82	25.70	30.42	1.038	.888	54.48	24.06	5.50	38.39	24.30	2.187	1.217	51.29	27.39
.91	25.79	30.36	1.063	.887	54.33	23.97	6.00	38.89	24.28	2.285	1.223	50.57	26.89
1.00	25.88	30.30	1.088	.883	54.18	23.88	6.50	39.39	24.17	2.374	1.228	49.86	26.39
1.20	26.08	30.18	1.138	.878	53.86	23.68	7.00	39.89	24.06	2.467	1.233	49.15	25.89
1.40	26.28	30.06	1.183	.873	53.54	23.48	7.50	40.39	23.95	2.563	1.237	48.44	25.39
1.60	26.48	29.94	1.222	.868	53.22	23.28	8.00	40.89	23.84	2.650	1.241	47.73	24.89
1.80	26.68	29.88	1.263	.863	52.96	23.08	9.00	41.89	22.42	2.842	1.247	46.31	23.89
							10.00	42.89	22.02	3.039	1.252	44.91	22.89
							11.00	43.89	21.63	3.242	1.255	43.52	21.89

TABLE I. - DETAILED NOZZLE DESIGN PARAMETERS - Continued

 $[\gamma = 1.400]$ 

1	2	3	4	5	6	7	1	2	3	4	5	6	7
$\gamma^-$ (deg)	$\gamma$ (deg)	$\beta$ (deg)	$\frac{x}{A_v/2}$	$\frac{y}{A_v/2}$	$\lambda^-$ (deg)	$\alpha$ (deg)	$\gamma^-$ (deg)	$\gamma$ (deg)	$\beta$ (deg)	$\frac{x}{A_v/2}$	$\frac{y}{A_v/2}$	$\lambda^-$ (deg)	$\alpha$ (deg)
$M_p, 4.00; \varphi$ and $\gamma_r^+, 32.89^\circ$							25.00	63.46	15.13	9.733	2.083	28.59	13.46
12.00	44.89	21.25	3.453	1.256	42.14	20.89	27.00	65.46	14.57	11.190	2.023	26.03	11.46
13.00	45.89	20.87	3.669	1.255	40.76	19.89	29.00	67.46	14.01	12.877	1.910	23.47	9.46
14.00	46.89	20.50	3.897	1.252	39.39	18.89	31.00	69.46	13.47	14.827	1.733	20.93	7.46
15.00	47.89	20.13	4.143	1.244	38.02	17.89	33.00	71.46	12.93	17.187	1.460	18.39	5.46
16.00	48.89	19.77	4.387	1.235	36.66	16.89	35.00	73.46	12.41	19.720	1.100	15.87	3.46
17.00	49.89	19.42	4.660	1.221	35.31	15.89	37.00	75.46	11.90	23.027	.547	13.36	1.46
18.00	50.89	19.09	4.932	1.204	33.98	14.89	38.46	76.92	11.54	25.867	0	11.54	0
19.00	51.89	18.73	5.227	1.183	32.62	13.89	$M_p, 6.00; \varphi$ and $\gamma_r^+, 42.48^\circ$						
21.00	53.89	18.07	5.866	1.129	29.96	11.89	0	42.48	22.20	0	1.000	-----	42.48
23.00	55.89	17.43	6.607	1.050	27.32	9.89	.01	42.49	22.19	.593	1.217	64.66	42.47
25.00	57.89	16.79	7.445	.939	24.68	7.89	.04	42.52	22.18	.777	1.283	64.62	42.44
27.00	59.89	16.19	8.402	.792	22.08	5.89	.07	42.55	22.17	.860	1.313	64.58	42.41
29.00	61.89	15.59	9.518	.587	19.48	3.89	.10	42.58	22.16	.923	1.337	64.54	42.38
31.00	63.89	15.01	10.770	.329	16.90	1.89	.13	42.61	22.15	.970	1.353	64.50	42.35
32.89	65.78	14.48	12.179	0	14.48	0	.16	42.64	22.13	1.010	1.367	64.45	42.32
$M_p, 5.00; \varphi$ and $\gamma_r^+, 38.46^\circ$							.19	42.67	22.12	1.047	1.380	64.41	42.29
0	38.46	23.88	0	1.000	-----	38.46	.25	42.73	22.09	1.100	1.400	64.32	42.23
.01	38.47	23.87	.560	1.143	62.32	38.45	.31	42.79	22.06	1.147	1.420	64.23	42.17
.04	38.50	23.86	.727	1.167	62.28	38.42	.37	42.85	22.04	1.193	1.433	64.15	42.11
.07	38.53	23.85	.800	1.207	62.24	38.39	.46	42.94	22.00	1.247	1.453	64.02	42.02
.10	38.56	23.84	.883	1.220	62.20	38.36	.55	43.03	21.97	1.297	1.470	63.90	41.93
.13	38.59	23.82	.907	1.233	62.15	38.33	.64	43.12	21.93	1.347	1.490	63.77	41.84
.16	38.62	23.81	.940	1.240	62.11	38.30	.73	43.21	21.90	1.387	1.503	63.65	41.75
.19	38.65	23.79	.973	1.250	62.06	38.27	.82	43.30	21.87	1.427	1.517	63.53	41.66
.25	38.71	23.77	1.027	1.263	61.98	38.21	.91	43.39	21.83	1.467	1.530	63.40	41.57
.31	38.77	23.74	1.070	1.273	61.89	38.15	1.00	43.48	21.80	1.500	1.543	63.28	41.48
.37	38.83	23.71	1.113	1.280	61.80	38.09	1.20	43.68	21.72	1.580	1.570	63.00	41.28
.46	38.92	23.67	1.160	1.293	61.67	38.00	1.40	43.88	21.64	1.647	1.593	62.72	41.08
.55	39.01	23.64	1.207	1.307	61.55	37.91	1.60	44.08	21.56	1.703	1.613	62.44	40.88
.64	39.10	23.60	1.253	1.320	61.42	37.82	1.80	44.28	21.48	1.770	1.637	62.16	40.68
.73	39.19	23.56	1.290	1.327	61.29	37.73	2.00	44.48	21.40	1.827	1.657	61.88	40.48
.82	39.28	23.52	1.330	1.337	61.16	37.64	2.40	44.88	21.26	1.937	1.693	61.34	40.08
.91	39.37	23.48	1.363	1.347	61.03	37.55	2.80	45.28	21.11	2.047	1.730	60.79	39.68
1.00	39.46	23.45	1.393	1.353	60.91	37.46	3.20	45.68	20.95	2.153	1.767	60.23	39.28
1.20	39.66	23.37	1.467	1.370	60.63	37.26	3.60	46.08	20.80	2.253	1.800	59.68	38.88
1.40	39.86	23.28	1.527	1.387	60.34	37.06	4.00	46.48	20.66	2.363	1.833	59.14	38.48
1.60	40.06	23.20	1.580	1.397	60.06	36.86	4.50	46.98	20.47	2.477	1.870	58.45	37.98
1.80	40.26	23.11	1.640	1.413	59.77	36.66	5.00	47.48	20.29	2.600	1.910	57.77	37.48
2.00	40.46	23.03	1.690	1.423	59.49	36.46	5.50	47.98	20.10	2.727	1.947	57.08	36.98
2.40	40.86	22.86	1.790	1.447	58.92	36.06	6.00	48.48	19.92	2.867	1.987	56.40	36.48
2.80	41.26	22.69	1.887	1.470	58.35	35.66	6.50	48.98	19.74	2.997	2.027	55.72	35.98
3.20	41.66	22.53	1.980	1.490	57.79	35.26	7.00	49.48	19.57	3.127	2.063	55.05	35.48
3.60	42.06	22.36	2.070	1.510	57.22	34.86	7.50	49.98	19.39	3.273	2.107	54.37	34.98
4.00	42.46	22.21	2.167	1.533	56.67	34.46	8.00	50.48	19.22	3.403	2.140	53.70	34.48
4.50	42.96	22.00	2.267	1.553	55.96	33.96	9.00	51.48	18.88	3.690	2.217	52.36	33.48
5.00	43.46	21.81	2.373	1.577	55.27	33.46	10.00	52.48	18.54	3.977	2.290	51.02	32.48
5.50	43.96	21.61	2.480	1.597	54.57	32.96	11.00	53.48	18.22	4.293	2.367	49.70	31.48
6.00	44.46	21.41	2.607	1.623	53.87	32.46	12.00	54.48	17.88	4.620	2.440	48.36	30.48
6.50	44.96	21.23	2.710	1.643	53.19	31.96	13.00	55.48	17.56	4.983	2.517	47.04	29.48
7.00	45.46	21.04	2.827	1.667	52.50	31.46	14.00	56.48	17.25	5.357	2.597	45.73	28.48
7.50	45.96	20.85	2.943	1.687	51.81	30.96	15.00	57.48	16.93	5.770	2.673	44.41	27.48
8.00	46.46	20.67	3.057	1.707	51.13	30.46	16.00	58.48	16.62	6.187	2.750	43.10	26.48
9.00	47.46	20.30	3.303	1.750	49.76	29.46	17.00	59.48	16.32	6.667	2.830	41.80	25.48
10.00	48.46	19.93	3.547	1.790	48.39	28.46	18.00	60.48	16.02	7.150	2.903	40.50	24.48
11.00	49.46	19.57	3.813	1.830	47.03	27.46	19.00	61.48	15.72	7.683	2.977	39.20	23.48
12.00	50.46	19.22	4.083	1.867	45.68	26.46	21.00	63.48	15.13	8.897	3.127	36.61	21.48
13.00	51.46	18.89	4.377	1.903	44.35	25.46	23.00	65.49	14.57	10.337	3.267	34.05	19.48
14.00	52.46	18.54	4.680	1.937	43.00	24.46	25.00	67.48	14.01	12.000	3.377	31.49	17.48
15.00	53.46	18.22	5.010	1.967	41.68	23.46	27.00	69.48	13.47	14.010	3.480	28.95	15.48
16.00	54.46	17.88	5.340	1.997	40.34	22.46	29.00	71.48	12.93	16.400	3.533	26.41	13.48
17.00	55.46	17.56	5.713	2.023	39.02	21.46	31.00	73.48	12.41	19.200	3.527	23.89	11.48
18.00	56.46	17.25	6.090	2.047	37.71	20.46	33.00	75.48	11.90	22.667	3.433	21.38	9.48
19.00	57.46	16.93	6.500	2.067	36.39	19.46	35.00	77.48	11.40	26.547	3.223	18.88	7.48
21.00	59.46	16.32	7.427	2.097	33.78	17.46	37.00	79.48	10.90	31.61	2.80	16.38	5.48
23.00	61.46	15.72	8.497	2.103	31.18	15.46	39.00	81.48	10.41	37.93	2.13	13.89	3.48
							41.00	83.48	9.95	46.03	1.06	11.43	1.48
							42.48	84.96	9.59	52.53	0	9.59	0





TABLE I. - DETAILED NOZZLE DESIGN PARAMETERS - Concluded

$$[\gamma = 1.400]$$

1	2	3	4	5	6	7	1	2	3	4	5	6	7
$\gamma^-$ (deg)	$\gamma$ (deg)	$\beta$ (deg)	$\frac{x}{A_t/2}$	$\frac{y}{A_t/2}$	$\lambda^-$ (deg)	$\alpha$ (deg)	$\gamma^-$ (deg)	$\gamma$ (deg)	$\beta$ (deg)	$\frac{x}{A_t/2}$	$\frac{y}{A_t/2}$	$\lambda^-$ (deg)	$\alpha$ (deg)
$M_f, 9.00; \varphi \text{ and } \gamma_f^+, 49.66^\circ$							$M_f, 10.00; \varphi \text{ and } \gamma_f^+, 51.16^\circ$						
0	49.66	19.50	0	1.000	-----	49.66	0	51.16	19.00	0	1.000	-----	51.16
.01	49.67	19.50	.673	1.387	69.15	49.65	.01	51.17	18.99	.690	1.430	70.14	51.15
.04	49.70	19.49	.880	1.507	69.11	49.62	.04	51.20	18.98	.900	1.560	70.10	51.12
.07	49.73	19.48	.970	1.560	69.07	49.59	.07	51.23	18.97	.993	1.620	70.06	51.09
.10	49.76	19.47	1.043	1.600	69.03	49.56	.10	51.26	18.96	1.070	1.667	70.02	51.06
.13	49.79	19.46	1.097	1.630	68.98	49.53	.13	51.29	18.95	1.123	1.700	69.98	51.03
.16	49.82	19.44	1.143	1.657	68.94	49.50	.16	51.32	18.94	1.173	1.730	69.94	51.00
.19	49.85	19.43	1.183	1.680	68.90	49.47	.19	51.35	18.93	1.213	1.757	69.90	50.97
.25	49.91	19.42	1.243	1.713	68.83	49.41	.25	51.41	18.91	1.273	1.793	69.82	50.91
.31	49.97	19.39	1.300	1.747	68.74	49.35	.31	51.47	18.88	1.333	1.827	69.73	50.85
.37	50.03	19.37	1.353	1.780	68.66	49.29	.37	51.53	18.86	1.390	1.863	69.65	50.79
.46	50.12	19.34	1.410	1.810	68.54	49.20	.46	51.62	18.83	1.447	1.897	69.53	50.70
.55	50.21	19.31	1.470	1.843	68.42	49.11	.55	51.71	18.80	1.507	1.937	69.41	50.61
.64	50.30	19.28	1.527	1.877	68.30	49.02	.64	51.80	18.77	1.567	1.973	69.29	50.52
.73	50.39	19.24	1.573	1.903	68.17	48.93	.73	51.89	18.73	1.617	2.003	69.16	50.43
.82	50.48	19.22	1.627	1.933	68.06	48.84	.82	51.98	18.71	1.667	2.033	69.05	50.34
.91	50.57	19.19	1.667	1.957	67.94	48.75	.91	52.07	18.68	1.713	2.060	68.93	50.25
1.00	50.66	19.16	1.710	1.980	67.82	48.66	1.00	52.16	18.65	1.757	2.090	68.81	50.16
1.20	50.86	19.10	1.800	2.030	67.56	48.46	1.20	52.36	18.58	1.853	2.147	68.54	49.96
1.40	51.06	19.04	1.880	2.077	67.30	48.26	1.40	52.56	18.51	1.933	2.197	68.27	49.76
1.60	51.26	18.96	1.953	2.117	67.02	48.06	1.60	52.76	18.45	2.007	2.240	68.01	49.56
1.80	51.46	18.89	2.033	2.160	66.75	47.86	1.80	52.96	18.39	2.090	2.290	67.75	49.36
2.00	51.66	18.82	2.100	2.200	66.48	47.66	2.00	53.16	18.33	2.160	2.333	67.49	49.16
2.40	52.06	18.68	2.237	2.273	66.94	47.26	2.40	53.56	18.19	2.303	2.417	66.95	48.76
2.80	52.46	18.54	2.377	2.350	66.40	46.86	2.80	53.96	18.05	2.447	2.500	66.41	48.36
3.20	52.86	18.42	2.507	2.420	64.88	46.46	3.20	54.36	17.92	2.580	2.582	65.88	47.96
3.60	53.26	18.29	2.637	2.487	64.35	46.06	3.60	54.76	17.79	2.720	2.657	65.35	47.56
4.00	53.66	18.16	2.773	2.560	63.82	45.66	4.00	55.16	17.67	2.863	2.740	64.83	47.16
4.50	54.16	17.99	2.927	2.640	63.15	45.16	4.50	55.66	17.50	3.023	2.830	64.16	46.66
5.00	54.66	17.82	3.087	2.720	62.48	44.66	5.00	56.16	17.35	3.197	2.927	63.51	46.16
5.50	55.16	17.67	3.250	2.803	61.83	44.16	5.50	56.66	17.19	3.370	3.020	62.85	45.66
6.00	55.66	17.50	3.440	2.897	61.16	43.66	6.00	57.16	17.03	3.567	3.127	62.19	45.16
6.50	56.16	17.35	3.610	2.983	60.51	43.16	6.50	57.66	16.87	3.750	3.223	61.53	44.66
7.00	56.66	17.19	3.793	3.070	59.85	42.66	7.00	58.16	16.71	3.943	3.323	60.87	44.16
7.50	57.16	17.03	3.987	3.160	59.19	42.16	7.50	58.66	16.56	4.153	3.430	60.22	43.66
8.00	57.66	16.87	4.170	3.247	58.53	41.66	8.00	59.16	16.41	4.347	3.533	59.57	43.16
9.00	58.66	16.56	4.530	3.410	57.22	40.66	9.00	60.16	16.11	4.730	3.723	58.27	42.16
10.00	59.66	16.26	4.943	3.590	55.92	39.66	10.00	61.16	15.81	5.180	3.947	56.97	41.16
11.00	60.66	15.96	5.400	3.787	54.62	38.66	11.00	62.16	15.51	5.683	4.190	55.67	40.16
12.00	61.66	15.66	5.877	3.980	53.32	37.66	12.00	63.16	15.21	6.213	4.433	54.37	39.16
13.00	62.66	15.36	6.413	4.190	52.02	36.66	13.00	64.16	14.93	6.907	4.700	53.09	38.16
14.00	63.66	15.07	6.983	4.410	50.73	35.66	14.00	65.16	14.65	7.440	4.977	51.81	37.16
15.00	64.66	14.79	7.613	4.643	49.45	34.66	15.00	66.16	14.38	8.147	5.273	50.54	36.16
16.00	65.66	14.51	8.273	4.873	48.17	33.66	16.00	67.16	14.10	8.890	5.573	49.26	35.16
17.00	66.66	14.24	9.013	5.120	46.90	32.66	17.00	68.16	13.82	9.733	5.900	47.98	34.16
18.00	67.66	13.96	9.800	5.377	45.62	31.66	18.00	69.16	13.56	10.640	6.243	46.72	33.16
19.00	68.66	13.69	10.680	5.653	44.35	30.66	19.00	70.16	13.28	11.613	6.583	45.44	32.16
21.00	70.66	13.15	12.693	6.240	41.81	28.66	21.00	72.16	12.75	13.893	7.323	42.91	30.16
23.00	72.66	12.62	15.183	6.887	39.28	26.66	23.00	74.16	12.24	16.723	8.167	40.40	28.16
25.00	74.66	12.11	18.200	7.600	36.77	24.66	25.00	76.16	11.72	20.190	9.103	37.98	26.16
27.00	76.66	11.60	21.960	8.577	34.26	22.66	27.00	78.16	11.23	24.507	10.140	35.39	24.16
29.00	78.66	11.10	26.533	9.190	31.76	20.66	29.00	80.16	10.74	29.98	11.30	32.90	22.16
31.00	80.66	10.61	32.20	10.04	29.27	18.66	31.00	82.16	10.26	36.67	12.57	30.42	20.16
33.00	82.66	10.15	39.47	10.96	26.81	16.66	33.00	84.16	9.77	45.37	13.97	27.93	18.16
35.00	84.66	9.66	48.15	11.83	24.32	14.66	35.00	86.16	9.32	55.88	15.38	25.48	16.16
37.00	86.66	9.20	59.91	12.70	21.86	12.66	37.00	88.16	8.84	69.87	16.77	23.00	14.16
39.00	88.66	8.73	74.92	13.56	19.39	10.66	39.00	90.16	8.39	88.35	18.18	20.55	12.16
41.00	90.66	8.28	93.92	13.72	16.94	8.66	41.00	92.16	7.95	112.30	19.43	18.11	10.16
43.00	92.66	7.84	121.83	13.50	14.50	6.66	43.00	94.16	7.50	147.52	20.30	15.66	8.16
45.00	94.66	7.39	157.95	12.27	12.05	4.66	45.00	96.16	7.05	193.30	20.20	13.22	6.16
47.00	96.66	6.95	211.03	9.00	9.61	2.66	47.00	98.16	6.63	262.5	18.1	10.79	4.16
49.00	98.66	6.52	250.0	5.5	7.18	.66	49.00	100.16	6.20	356.2	12.9	8.36	2.16
49.66	99.32	6.38	306.7	0	6.38	0	51.16	102.32	5.74	509.7	0	5.74	0

TABLE II. - OVER-ALL NOZZLE DESIGN PARAMETERS

$$[\gamma = 1.400]$$



1	2	3	4	5	1	2	3	4	5
$M_f$	$\phi$ and $\psi_f^+$ (deg)	$\psi_f, \psi$ (deg)	$A_f/A_t$	$\beta_f, \beta$ (deg)	$M_f$	$\phi$ and $\psi_f^+$ (deg)	$\psi_f, \psi$ (deg)	$A_f/A_t$	$\beta_f, \beta$ (deg)
1.00	0	0	1.0000	90.000	1.80	10.362	20.725	1.4390	33.749
1.02	.063	.126	1.0003	78.635	1.82	10.652	21.304	1.4610	33.329
1.04	.175	.351	1.0013	74.058	1.84	10.939	21.878	1.4836	32.921
1.06	.318	.637	1.0029	70.630	1.86	11.225	22.450	1.5069	32.523
1.08	.484	.968	1.0051	67.808	1.88	11.510	23.020	1.5307	32.135
1.10	.668	1.336	1.0079	65.380	1.90	11.793	23.586	1.5553	31.757
1.12	.867	1.735	1.0113	63.234	1.92	12.076	24.152	1.5804	31.388
1.14	1.080	2.160	1.0153	61.306	1.94	12.356	24.713	1.6062	31.028
1.16	1.304	2.607	1.0198	59.550	1.96	12.635	25.270	1.6326	30.677
1.18	1.537	3.074	1.0248	57.936	1.98	12.913	25.827	1.6597	30.335
1.20	1.779	3.558	1.0304	56.443	2.00	13.190	26.380	1.6875	30.000
1.22	2.028	4.057	1.0366	55.052	2.02	13.464	26.929	1.7160	29.673
1.24	2.285	4.570	1.0432	53.751	2.04	13.738	27.476	1.7451	29.353
1.26	2.546	5.093	1.0504	52.528	2.06	14.011	28.022	1.7750	29.041
1.28	2.814	5.627	1.0581	51.375	2.08	14.281	28.562	1.8056	28.736
1.30	3.085	6.170	1.0663	50.285	2.10	14.548	29.097	1.8369	28.437
1.32	3.360	6.721	1.0750	49.251	2.12	14.815	29.631	1.8690	28.145
1.34	3.635	7.279	1.0842	48.268	2.14	15.080	30.161	1.9018	27.859
1.36	3.922	7.844	1.0940	47.332	2.16	15.344	30.688	1.9354	27.578
1.38	4.206	8.413	1.1042	46.439	2.18	15.606	31.213	1.9698	27.304
1.40	4.493	8.987	1.1149	45.585	2.20	15.866	31.732	2.0050	27.036
1.42	4.782	9.565	1.1262	44.767	2.22	16.125	32.250	2.0409	26.773
1.44	5.073	10.146	1.1379	43.983	2.24	16.381	32.763	2.0777	26.515
1.46	5.365	10.730	1.1502	43.230	2.26	16.637	33.274	2.1154	26.262
1.48	5.663	11.327	1.1629	42.507	2.28	16.889	33.778	2.1538	26.014
1.50	5.953	11.906	1.1762	41.810	2.30	17.141	34.283	2.1931	25.772
1.52	6.248	12.495	1.1899	41.140	2.32	17.391	34.782	2.2333	25.533
1.54	6.542	13.085	1.2042	40.493	2.34	17.639	35.279	2.2744	25.300
1.56	6.837	13.675	1.2190	39.868	2.36	17.885	35.771	2.3164	25.070
1.58	7.135	14.270	1.2344	39.265	2.38	18.131	36.262	2.3593	24.845
1.60	7.430	14.860	1.2502	38.682	2.40	18.373	36.746	2.4031	24.624
1.62	7.726	15.452	1.2666	38.118	2.42	18.615	37.230	2.4479	24.407
1.64	8.021	16.043	1.2835	37.572	2.44	18.854	37.708	2.4936	24.195
1.66	8.316	16.633	1.3010	37.043	2.46	19.092	38.184	2.5403	23.985
1.68	8.611	17.223	1.3190	36.530	2.48	19.327	38.655	2.5880	23.780
1.70	8.905	17.810	1.3376	36.032	2.50	19.562	39.124	2.6367	23.578
1.72	9.198	18.397	1.3567	35.549	2.52	19.794	39.589	2.6864	23.380
1.74	9.490	18.981	1.3764	35.080	2.54	20.025	40.050	2.7372	23.185
1.76	9.783	19.566	1.3967	34.624	2.56	20.254	40.508	2.7891	22.993
1.78	10.073	20.146	1.4175	34.180	2.58	20.481	40.963	2.8420	22.805

TABLE II. - OVER-ALL NOZZLE DESIGN PARAMETERS - Continued  
 $[\gamma = 1.400]$

1	2	3	4	5	1	2	3	4	5
$M_f$	$\phi$ and $\psi_f^+$ (deg)	$\psi_f, \psi$ (deg)	$A_f/A_t$	$\beta_f, \beta$ (deg)	$M_f$	$\phi$ and $\psi_f^+$ (deg)	$\psi_f, \psi$ (deg)	$A_f/A_t$	$\beta_f, \beta$ (deg)
2.60	20.707	41.415	2.8960	22.620	3.30	27.611	55.222	5.6286	17.640
2.62	20.931	41.863	2.9511	22.438	3.32	27.782	55.564	5.7358	17.530
2.64	21.154	42.308	3.0073	22.259	3.34	27.952	55.904	5.8448	17.422
2.66	21.374	42.749	3.0647	22.082	3.36	28.120	56.241	5.9558	17.315
2.68	21.593	43.187	3.1233	21.909	3.38	28.288	56.576	6.0687	17.209
2.70	21.810	43.621	3.1830	21.738	3.40	28.454	56.908	6.1837	17.105
2.72	22.026	44.053	3.2440	21.571	3.42	28.619	57.238	6.3007	17.002
2.74	22.240	44.481	3.3061	21.405	3.44	28.782	57.564	6.4198	16.900
2.76	22.453	44.906	3.3695	21.243	3.46	28.944	57.888	6.5409	16.799
2.78	22.664	45.328	3.4342	21.082	3.48	29.105	58.210	6.6642	16.700
2.80	22.873	45.746	3.5001	20.925	3.50	29.265	58.530	6.7896	16.602
2.82	23.080	46.161	3.5674	20.770	3.52	29.973	58.847	6.9172	16.504
2.84	23.286	46.573	3.6359	20.617	3.54	29.581	59.162	7.0470	16.409
2.86	23.491	46.982	3.7058	20.466	3.56	29.737	59.474	7.1791	16.314
2.88	23.694	47.388	3.7771	20.318	3.58	29.892	59.784	7.3135	16.220
2.90	23.895	47.790	3.8498	20.171	3.60	30.045	60.091	7.4501	16.128
2.92	24.095	48.190	3.9238	20.027	3.62	30.198	60.397	7.5891	16.036
2.94	24.293	48.586	3.9993	19.885	3.64	30.350	60.700	7.7304	15.946
2.96	24.490	48.980	4.0763	19.745	3.66	30.500	61.000	7.8742	15.856
2.98	24.685	49.370	4.1547	19.607	3.68	30.649	61.299	8.0204	15.768
3.00	24.878	49.757	4.2346	19.471	3.70	30.747	61.595	8.1690	15.680
3.02	25.071	50.142	4.3160	19.337	3.72	30.944	61.889	8.3202	15.594
3.04	25.261	50.523	4.3989	19.205	3.74	31.090	62.181	8.4739	15.508
3.06	25.451	50.902	4.4835	19.074	3.76	31.235	62.471	8.6302	15.424
3.08	25.638	51.277	4.5696	18.946	3.78	31.379	62.758	8.7891	15.340
3.10	25.825	51.650	4.6573	18.819	3.80	31.522	63.044	8.9506	15.258
3.12	26.010	52.020	4.7467	18.694	3.82	31.663	63.327	9.1148	15.176
3.14	26.193	52.386	4.8377	18.570	3.84	31.804	63.608	9.2817	15.095
3.16	26.375	52.750	4.9304	18.449	3.86	31.943	63.887	9.4513	15.015
3.18	26.556	53.112	5.0248	18.328	3.88	32.082	64.164	9.6237	14.936
3.20	26.735	53.470	5.1210	18.210	3.90	32.220	64.440	9.7990	14.857
3.22	26.913	53.826	5.2189	18.093	3.92	32.356	64.713	9.9771	14.780
3.24	27.089	54.179	5.3186	17.977	3.94	32.492	64.984	10.1580	14.703
3.26	27.265	54.530	5.4201	17.863	3.96	32.626	65.253	10.3420	14.627
3.28	27.438	54.877	5.5234	17.751	3.98	32.760	65.520	10.5288	14.552

TABLE II. - OVER-ALL NOZZLE DESIGN PARAMETERS - Continued  
 $[\gamma = 1.400]$

1	2	3	4	5	1	2	3	4	5
$M_f$	$\phi$ and $\psi_f^+$ (deg)	$\psi_f, \psi$ (deg)	$A_f/A_t$	$\beta_f, \beta$ (deg)	$M_f$	$\phi$ and $\psi_f^+$ (deg)	$\psi_f, \psi$ (deg)	$A_f/A_t$	$\beta_f, \beta$ (deg)
4.00	32.892	65.785	10.719	14.478	5.50	40.622	81.244	36.869	10.476
4.05	33.219	66.439	11.207	14.295	5.55	40.821	81.643	38.281	10.380
4.10	33.542	67.085	11.715	14.117	5.60	41.016	82.032	39.741	10.287
4.15	33.857	67.714	12.243	13.943	5.65	41.209	82.418	41.246	10.195
4.20	34.167	68.334	12.791	13.774	5.70	41.397	82.795	42.796	10.104
4.25	34.472	68.945	13.363	13.609	5.75	41.585	83.171	44.400	10.015
4.30	34.770	69.541	13.955	13.448	5.80	41.768	83.537	46.050	9.928
4.35	35.064	70.128	14.571	13.290	5.85	41.950	83.900	47.754	9.842
4.40	35.353	70.707	15.210	13.137	5.90	42.128	84.257	49.507	9.758
4.45	35.637	71.274	15.874	12.986	5.95	42.303	84.607	51.318	9.675
4.50	35.916	71.833	16.562	12.840	6.00	42.477	84.955	53.178	9.594
4.55	36.190	72.380	17.277	12.696	6.05	42.649	85.299	55.101	9.514
4.60	36.459	72.919	18.018	12.556	6.10	42.817	85.634	57.077	9.435
4.65	36.724	73.448	18.787	12.419	6.15	42.984	85.968	59.114	9.358
4.70	36.984	73.969	19.583	12.284	6.20	43.148	86.296	61.210	9.282
4.75	37.241	74.483	20.409	12.153	6.25	43.309	86.618	63.370	9.207
4.80	37.493	74.986	21.263	12.025	6.30	43.469	86.938	65.589	9.133
4.85	37.741	75.483	22.151	11.899	6.35	43.625	87.251	67.877	9.061
4.90	37.985	75.970	23.067	11.776	6.40	43.780	87.561	70.228	8.989
4.95	38.225	76.451	24.018	11.655	6.45	43.934	87.868	72.647	8.919
5.00	38.460	76.921	25.000	11.537	6.50	44.084	88.169	75.134	8.850
5.05	38.691	77.383	26.018	11.421	6.55	44.233	88.466	77.695	8.782
5.10	38.920	77.841	27.069	11.308	6.60	44.379	88.759	80.323	8.715
5.15	39.146	78.293	28.159	11.197	6.65	44.525	89.051	83.027	8.649
5.20	39.367	78.735	29.283	11.088	6.70	44.668	89.336	85.804	8.584
5.25	39.585	79.170	30.446	10.981	6.75	44.809	89.618	88.661	8.520
5.30	39.799	79.599	31.649	10.876	6.80	44.947	89.895	91.594	8.457
5.35	40.008	80.017	32.893	10.773	6.85	45.085	90.170	94.609	8.394
5.40	40.216	80.433	34.174	10.672	6.90	45.221	90.442	97.700	8.333
5.45	40.422	80.844	35.501	10.573	6.95	45.355	90.710	100.880	8.273

TABLE II. - OVER-ALL NOZZLE DESIGN PARAMETERS - Concluded  
 $[\gamma = 1.400]$

1	2	3	4	5	1	2	3	4	5
$M_f$	$\phi$ and $\psi_f^+$ (deg)	$\psi_f', \psi$ (deg)	$A_f/A_t$	$\beta_f, \beta$ (deg)	$M_f$	$\phi$ and $\psi_f^+$ (deg)	$\psi_f', \psi$ (deg)	$A_f/A_t$	$\beta_f, \beta$ (deg)
7.00	45.487	90.974	104.143	8.213	8.50	48.786	97.573	251.086	6.756
7.05	45.618	91.237	107.492	8.155	8.55	48.878	97.757	257.974	6.717
7.10	45.746	91.492	110.931	8.097	8.60	48.969	97.938	265.014	6.677
7.15	45.873	91.746	114.459	8.040	8.65	49.059	98.118	272.211	6.639
7.20	45.999	91.999	118.080	7.984	8.70	49.147	98.294	279.567	6.600
7.25	46.122	92.244	121.794	7.928	8.75	49.234	98.469	287.084	6.562
7.30	46.245	92.491	125.605	7.873	8.80	49.321	98.643	294.766	6.525
7.35	46.365	92.731	129.513	7.820	8.85	49.407	98.814	302.615	6.488
7.40	46.485	92.971	133.520	7.766	8.90	49.491	98.983	310.633	6.451
7.45	46.603	93.206	137.629	7.714	8.95	49.576	99.153	318.823	6.415
7.50	46.720	93.441	141.842	7.662	9.00	49.660	99.320	327.190	6.379
7.55	46.835	93.671	146.159	7.611	9.05	49.741	99.483	335.733	6.344
7.60	46.949	93.898	150.585	7.561	9.10	49.823	99.647	344.458	6.309
7.65	47.061	94.122	155.120	7.511	9.15	49.904	99.808	353.368	6.274
7.70	47.172	94.345	159.770	7.462	9.20	49.983	99.967	362.463	6.240
7.75	47.283	94.567	164.527	7.414	9.25	50.063	100.127	371.749	6.206
7.80	47.391	94.783	169.403	7.366	9.30	50.141	100.282	381.228	6.173
7.85	47.499	94.998	174.418	7.319	9.35	50.219	100.438	390.902	6.140
7.90	47.604	95.209	179.511	7.272	9.40	50.295	100.591	400.775	6.107
7.95	47.708	95.417	184.744	7.226	9.45	50.371	100.742	410.851	6.074
8.00	47.813	95.627	190.109	7.181	9.50	50.445	100.891	421.131	6.042
8.05	47.916	95.832	195.597	7.136	9.55	50.520	101.041	431.620	6.011
8.10	48.016	96.033	201.215	7.092	9.60	50.594	101.188	442.322	5.979
8.15	48.117	96.234	206.964	7.048	9.65	50.667	101.334	453.236	5.948
8.20	48.215	96.431	212.846	7.005	9.70	50.738	101.476	464.370	5.917
8.25	48.312	96.625	218.865	6.962	9.75	50.811	101.623	475.725	5.887
8.30	48.410	96.821	225.022	6.920	9.80	50.882	101.764	487.304	5.857
8.35	48.506	97.013	231.320	6.878	9.85	50.951	101.903	499.112	5.827
8.40	48.599	97.199	237.763	6.837	9.90	51.021	102.042	511.152	5.797
8.45	48.694	97.388	244.350	6.796	9.95	51.090	102.180	523.425	5.768
					10.00	51.158	102.317	535.938	5.739



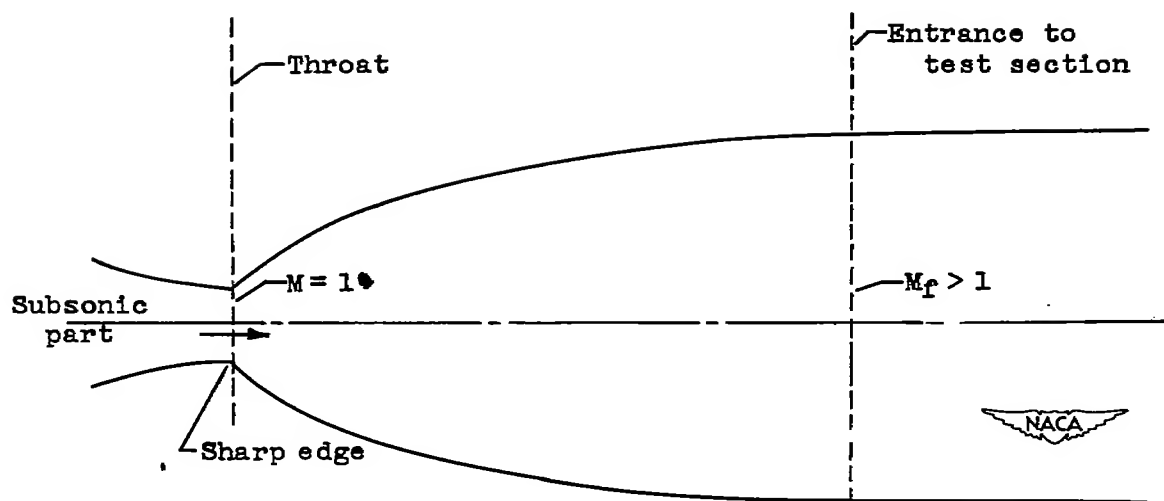
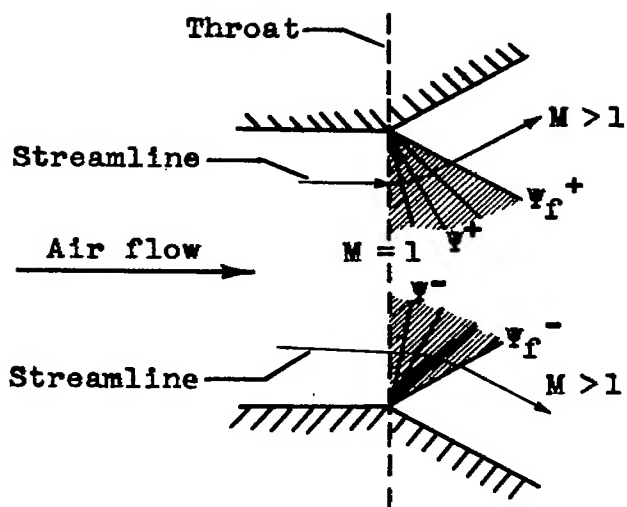
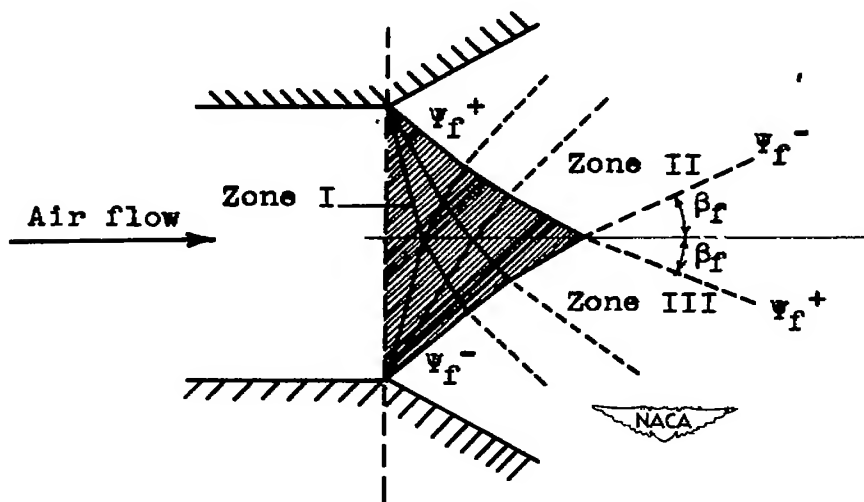


Figure 1. - Sharp-edge-throat supersonic nozzle of minimum length.



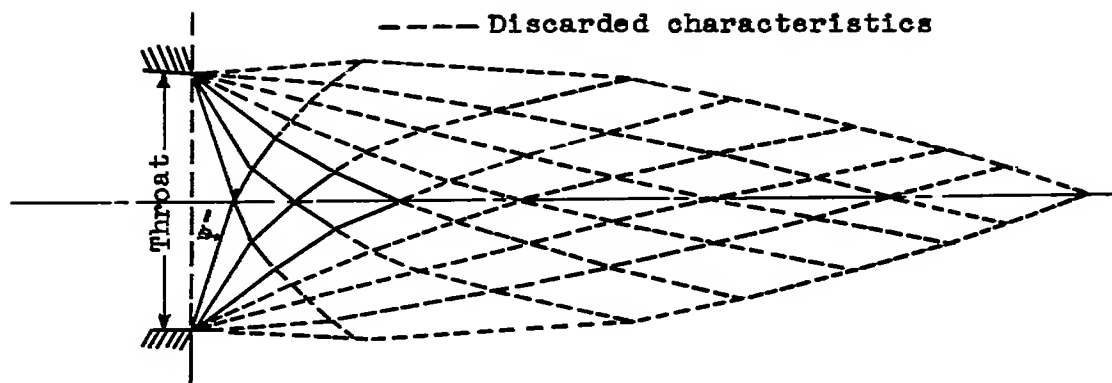
(a) Expansion waves represented by a finite number of characteristics.



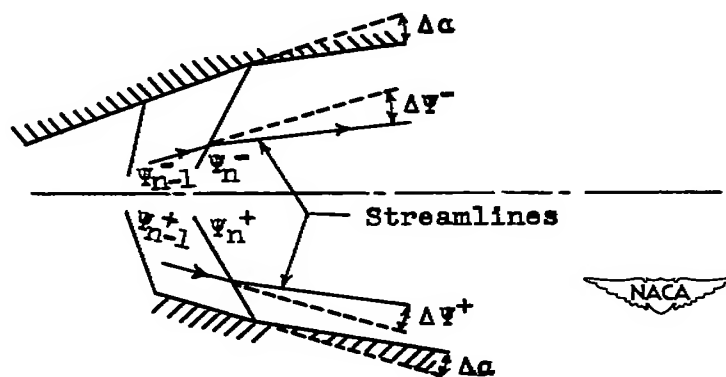
(b) Wave pattern formed by interaction of two expansion waves.

Figure 2. - Schematic representation of expansion waves by characteristics.



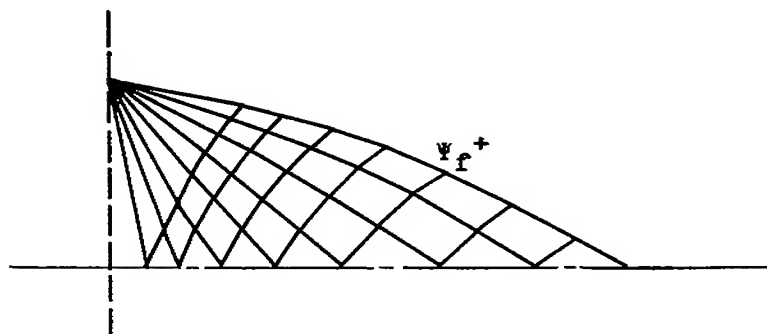


(c) Kernel formed from kernel corresponding to higher Mach number.

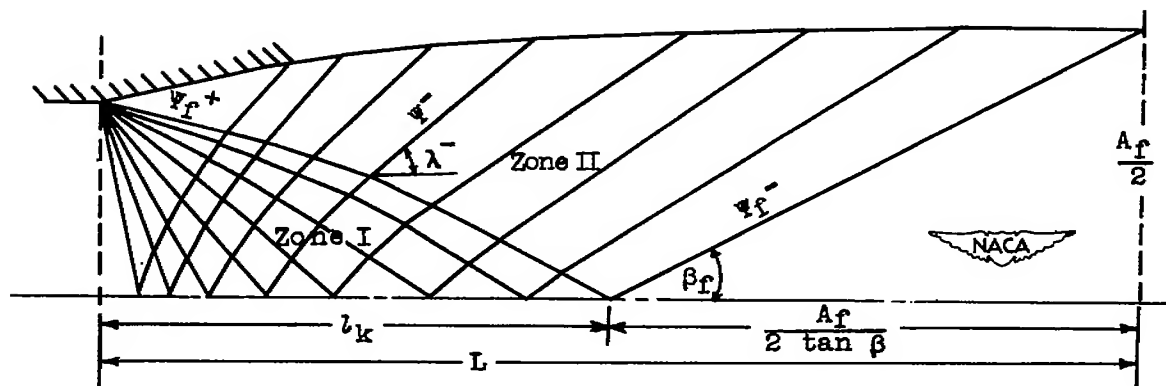


(d) Suppression of expansion wave by bending wall.

Figure 2. - Concluded. Schematic representation of expansion waves by characteristics.

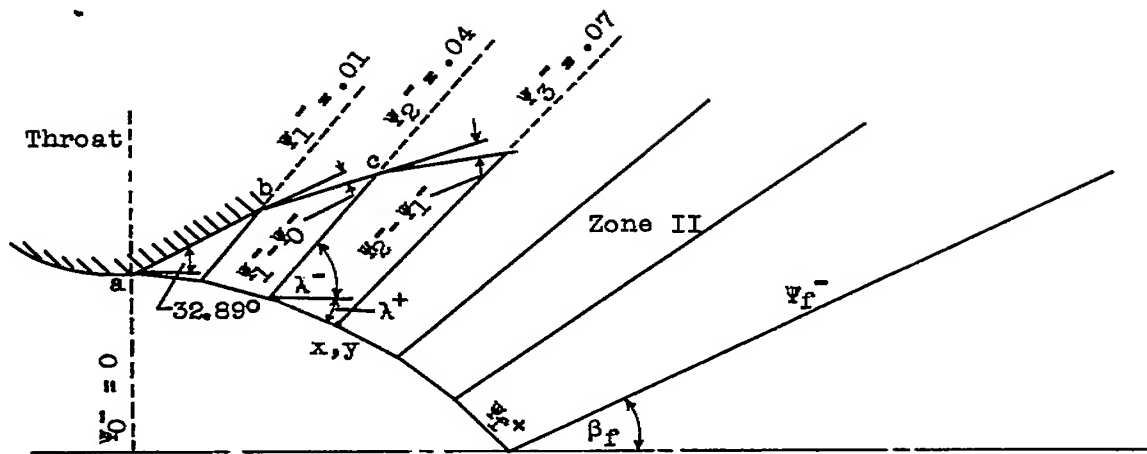


(a) Kernel.

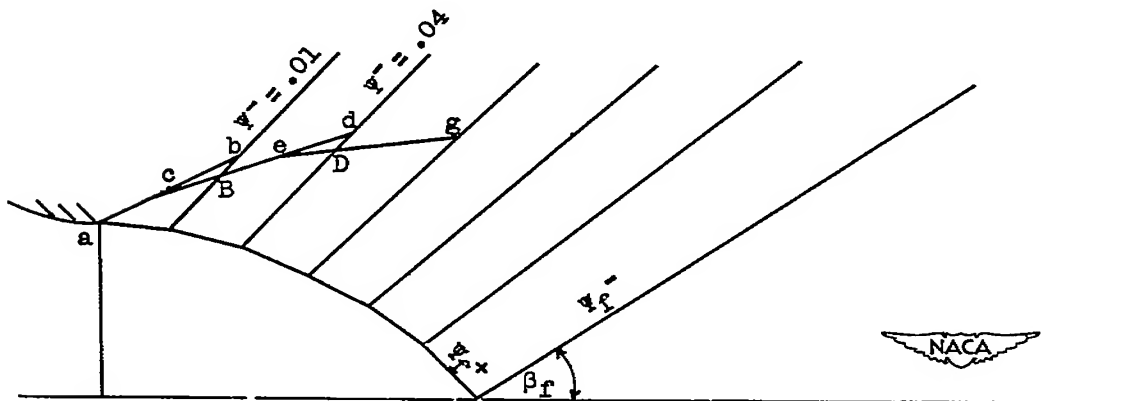


(b) Wave pattern and wall contour.

Figure 3. - Complete wave pattern and wall contour of graphically designed nozzle with sharp-edge throat.



(a) Conventional development.



(b) Averaging development.

Figure 4. - Development of wall contour from bounding  $\psi_f^+$  characteristic of kernel.

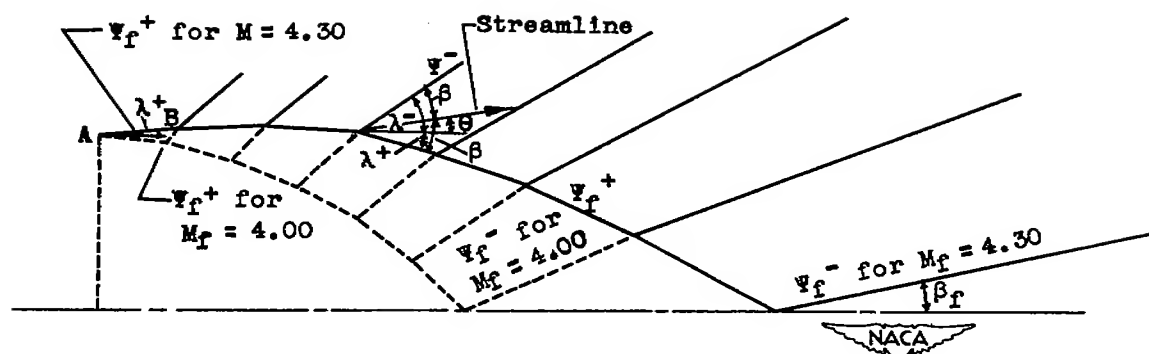


Figure 5. - Method of determining bounding characteristic  $\Psi_f^+$  for a desired Mach number from a known adjacent characteristic.

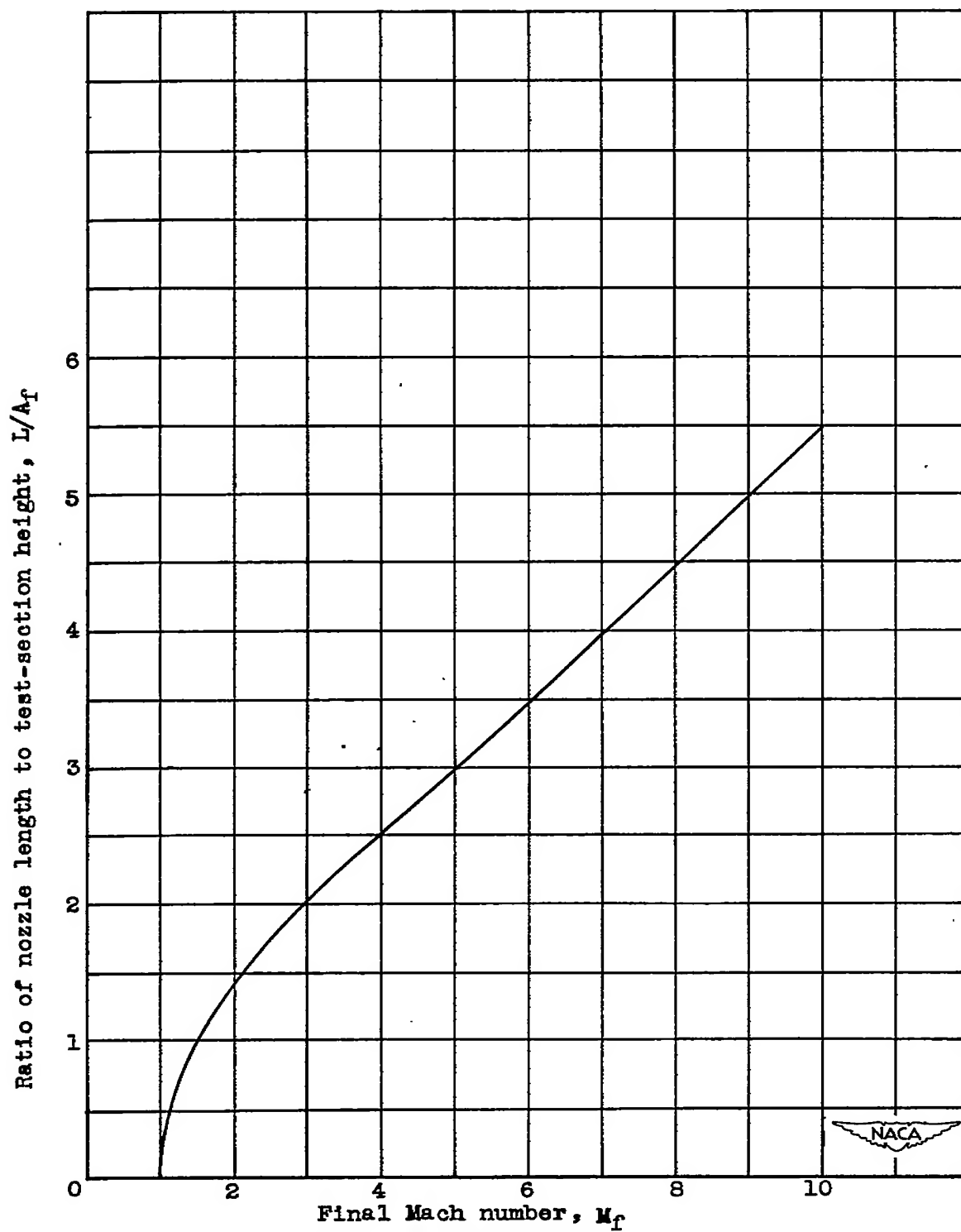


Figure 6. - Length of sharp-edge-throat nozzles.